Letter

Enhancing the Josephson diode effect with Majorana bound states

Jorge Cayao,[1] Naoto Nagaosa,[2] and Yukio Tanaka[3,4]
[1]*Department of Physics and Astronomy, Uppsala University, Box 516, S-751 20 Uppsala, Sweden*
[2]*Center for Emergent Matter Science (CEMS), RIKEN, Wako, Saitama 351-0198, Japan*
[3]*Department of Applied Physics, Nagoya University, Nagoya 464–8603, Japan*
[4]*Research Center for Crystalline Materials Engineering, Nagoya University, Nagoya 464-8603, Japan*

(Received 4 October 2023; accepted 8 February 2024; published 26 February 2024)

We consider phase-biased Josephson junctions with spin-orbit coupling under external magnetic fields and study the emergence of the Josephson diode effect in the presence of Majorana bound states. We show that junctions having middle regions with Zeeman fields along the spin-orbit axis develop a low-energy Andreev spectrum that is asymmetric with respect to the superconducting phase difference $\phi = \pi$, which is strongly influenced by Majorana bound states in the topological phase. This asymmetric Andreev spectrum gives rise to anomalous current-phase curves and critical currents that are different for positive and negative supercurrents, thus signaling the emergence of the Josephson diode effect. While this effect exists even in the trivial phase, it gets enhanced in the topological phase due to the spatial nonlocality of Majorana bound states. Our paper thus establishes the utilization of topological superconductivity for enhancing the functionalities of Josephson diodes.

DOI: 10.1103/PhysRevB.109.L081405

Introduction. Diodes are devices that conduct current primarily along one direction and constitute key building blocks of numerous electronic components [1–6]. Diodes have been initially studied in the normal state [7,8], where inevitable energy losses appear due to finite resistance. This issue has been resolved in superconductors (Ss), which showed superior diode functionalities [9–11], with dissipationless supercurrents in bulk systems [12–20] and in Josephson junctions (JJs) [21–28]. Of particular interest are diodes in JJs, known as Josephson diodes (JDs), because supercurrents here are controlled by virtue of the Josephson effect, which arises due to the finite phase difference between coupled Ss [29,30]. This phase also enables the formation of Andreev bound states (ABSs), which determine the profile of supercurrents [31–41] and reveal the nature of emergent superconductivity [42–53].

Most of the studies on JDs have involved systems with spin-orbit coupling (SOC) and magnetic fields, with experiments that strongly support their realization in semiconductor-S junctions [14,22,54–56]. Moreover, JDs are characterized based on their quality factors, which measure the diode's ability to conduct current along one direction. In this regard, recent studies have reported sizable and highly tunable quality factors, showing that JJs with SOC and magnetism hold great promise for JDs.

Superconductors with SOC under magnetic fields have also been explored for realizing topological superconductivity [42,50–53,57–61], a topological state that hosts Majorana bound states (MBSs) and promises to revolutionize future quantum technologies. MBSs emerge above a critical magnetic field as charge-neutral topologically protected quasiparticles and exhibit spatial nonlocality [62–66], properties that have been recently explored in JJs [67–75] and shown to offer a solid way for topological qubits [76–80]. The spatial nonlocality occurs as a result of MBSs emerging spatially separated, which allows to store information in a nonlocal manner and immune against local sources of decoherence [76]. While the detection of MBSs has recently attracted a lot of interest [50–53], the realization of JDs in topological Ss with MBSs has received very limited attention so far [81–86]. In particular, it is still unknown how JDs respond to the Majorana nonlocality, an open question that could establish the realization and use of JDs for topological quantum phenomena.

In this paper we consider S-normal-S (SNS) JJs with SOC and Zeeman fields, and discover the emergence of highly tunable JDs, which acquire quality factors that are greatly enhanced by MBSs, specially, when they become more nonlocal. We find that these topological JDs occur when the middle N region has a Zeeman field component parallel to the SOC, which induces an asymmetric phase-dependent Andreev spectrum that gives rise to supercurrents with nonreciprocal behavior defining the JDs. While JDs can occur even in the trivial regime, it is only in the topological phase that they exhibit a strong dependence on the Majorana nonlocality, thus establishing the potential of MBSs for designing JDs with topologically protected and enhanced properties.

JJs based on nanowires. We consider SNS JJs formed on a single channel nanowire with Rashba SOC [Fig. 1(a)], with a continuum model given by

$$H = \xi_{p_x}\tau_z + \frac{\alpha}{\hbar}p_x\sigma_y\tau_z + \Delta(x)\sigma_y\tau_y + H_Z(x), \qquad (1)$$

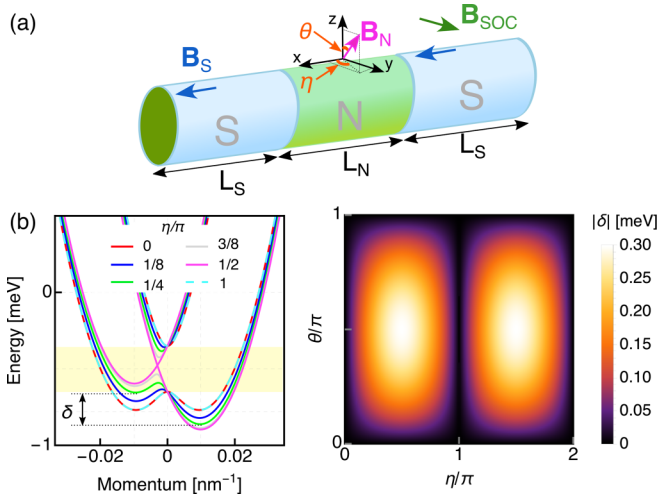

FIG. 1. (a) A JJ based on a nanowire with SOC field $\mathbf{B}_{\mathrm{SOC}}$ along y axis (green), with the N(S) region of length $L_{\mathrm{N(S)}}$. The N (S) region has a Zeeman field $\mathbf{B}_{\mathrm{N(S)}}$ with components perpendicular and parallel (only perpendicular) to $\mathbf{B}_{\mathrm{SOC}}$, see magenta (blue) arrow. (b) (Left) Energy vs momentum without superconductivity: while a perpendicular Zeeman field opens a gap at zero momentum (yellow region), a parallel term induces an asymmetry in the bands δ seen by fixing the angle of $\mathbf{B}_{\mathrm{N}}$ with the z axis to $\theta = \pi/2$ and varying the angle from the x axis η; δ is shown for $\eta = \pi/4$. The solid red ($\eta = 0$) and dashed cyan curves ($\eta = \pi$) are superimposed. (Right) δ at the SOC momenta as a function of θ and η. Parameters: $B_{\mathrm{N}} = 0.15$ meV, $\alpha = 40$ meVnm, $\mu = 0.5$ meV.

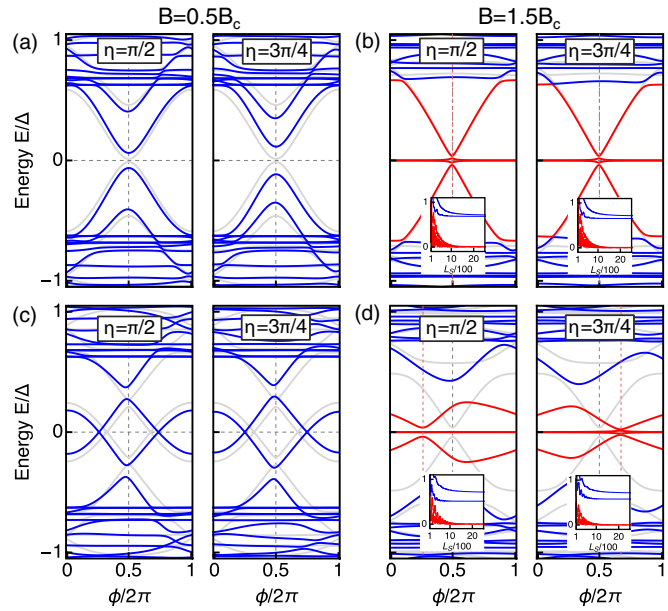

FIG. 2. Low-energy spectrum of JJs with $L_{\mathrm{N}} = 20$ nm [(a),(b)] and $L_{\mathrm{N}} = 100$ nm [(c),(d)] as a function of ϕ for $B < B_c$ and $B > B_c$ at different η. In (b) and (d) the nearest levels to zero are depicted in red color, while insets show the lowest four positive levels as function of L_{S}. Vertical-dashed lines mark where four MBSs appear. Gray curves in all panels correspond to $\eta = 0$. Parameters: $\alpha = 40$ meVnm, $\mu = 0.5$ meV, $\theta = \pi/2$, $L_{\mathrm{S}} = 1000$ nm, $\Delta = 0.5$ meV, $B_{\mathrm{N}} = 0.5$ meV.

where $\xi_{p_x} = p_x^2/(2m) - \mu$ is the kinetic part, $p_x = -i\hbar\partial_x$ is the momentum operator, μ is the chemical potential, α is the Rashba SOC strength, $H_Z(x)$ is the space dependent Zeeman field, $\Delta(x)$ the induced space dependent s-wave pair potential, and σ_i and τ_i are the ith Pauli matrices in spin and electron-hole spaces, respectively. For computational purposes, Eq. (1) is discretized into a tight-binding lattice with spacing $a = 10$ nm and then divided into three regions (left/right S and middle N) of finite lengths $L_{\mathrm{S,N}}$ [71,74], see Fig. 1(a). The S regions have a finite pair potential Δ with a phase difference ϕ, while N has $\Delta = 0$, originating a SNS JJ. To ensure that JD effect and MBSs can coexist, the Zeeman field is taken as $H_Z(x) = \mathbf{B}_{\mathrm{S(N)}} \cdot \mathbf{\Sigma}$, where $\mathbf{\Sigma} = (\sigma_x\tau_z, \sigma_y, \sigma_z\tau_z)$, $\mathbf{B}_{\mathrm{S}} = (B, 0, 0)$, and $\mathbf{B}_{\mathrm{N}} = B_{\mathrm{N}}(\sin\theta\cos\eta, \sin\theta\sin\eta, \cos\theta)$ [87], with $\theta \in (0, \pi)$ and $\eta \in (0, 2\pi)$. Moreover, we consider realistic parameters, with $\alpha_{\mathrm{R}} = 40$ meVnm and $\Delta = 0.5$ meV, according to experimental values reported for InSb and InAs nanowires and Nb and Al Ss [50].

The role of the Zeeman field can be already seen in the normal state, by inspecting the bands of Eq. (1) with $\Delta = 0$ and $\mathbf{B}_{\mathrm{N}}$. While a component of $\mathbf{B}_{\mathrm{N}}$ perpendicular to the SOC opens a gap at zero momentum $k = 0$ (yellow region), the band dispersion becomes asymmetric with respect to $k = 0$ when $\mathbf{B}_{\mathrm{N}}$ has a term parallel to SOC, see left panel of Fig. 1(b). This asymmetry can be characterized by the difference between the lowest bands at the SOC momenta $\pm m\alpha/\hbar^2$, denoted by δ, which gets a maximum at $\theta = \eta = \pi/2$ [Fig. 1(b)]. Below we will see that this asymmetry is crucial for achieving nonreciprocal Andreev spectrum and JDs in JJs.

Nonreciprocal phase-dependent Andreev spectrum. To start, we focus on the Andreev spectrum, which is presented in Fig. 2 as a function of ϕ for JJs with $L_{\mathrm{N}} = 20$ nm and $L_{\mathrm{N}} = 100$ nm at distinct η and B. The Andreev spectrum strongly depends on ϕ, revealing the appearance of ABSs within the induced gap, with interesting dependencies on η, L_{N}, and B. At $\eta = 0$, i.e., when $\mathbf{B}_{\mathrm{N}}$ is perpendicular to the SOC, the spectrum is symmetric with respect to $\phi = \pi$, see gray curves in Fig. 2. Here, $B = B_{\mathrm{c}}$, with $B_{\mathrm{c}} = \sqrt{\mu^2 + \Delta^2}$, defines a topological phase transition into a topological phase ($B > B_{\mathrm{c}}$) with four topological ABSs that depend on ϕ [67,70,88]. Correspondingly, for $B < B_{\mathrm{c}}$ the system is in the trivial phase and hosts two pairs of conventional spin-split ABSs having a cosine-like dependence on ϕ [34,40]. The topological ABSs at $\phi = \pi$ define four MBSs, two at the outer sides of S and two at their inner sides, while the ABSs at $\phi = 0$ only two MBSs located at two outer sides of the S regions [67,70,88]. For JJs with short Ss, the four MBSs split around zero energy at $\phi = \pi$, thus giving rise to a Majorana zero-energy splitting, which gets suppressed for long S regions and can be thus seen as a signal of the Majorana spatial nonlocality [72,74].

When $\mathbf{B}_{\mathrm{N}}$ acquires a component that is parallel to the SOC, characterized here by $\eta \neq 0$, the low-energy spectrum becomes highly asymmetric with respect to $\phi = \pi$ and develops important differences from the $\eta = 0$ case in both the topological and trivial phases [Figs. 2(c) and 2(d)]. The asymmetry is reflected in the in-gap ABSs, which involve MBSs in the topological phase, and also in the quasicontinuum above the induced gap. For JJs with $L_{\mathrm{N}} = 20$ nm and $\eta \neq 0$

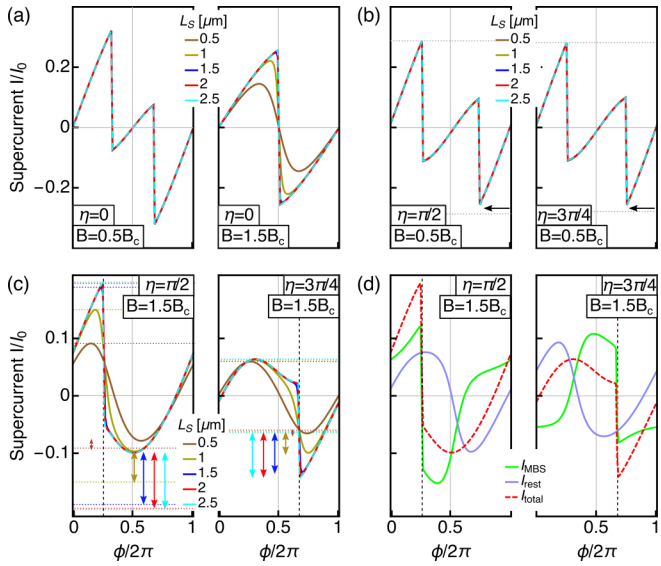

FIG. 3. (a) Supercurrents $I(\phi)$ in JJs with $L_N = 100$ nm as a function of ϕ at $\eta = 0$ for $B < B_c$ and $B > B_c$ and different L_S. (b,c) same as (a) but at $\eta = \pi/2, 3\pi/4$. Horizontal dotted lines mark $\pm I_c^+$; arrows in (b,d) indicate that $I_c^+ \neq I_c^-$. (d) Contributions of the four MBSs and the rest of levels (ABSs and quasicontinuum) to the total $I(\phi)$ for $L_S = 2$ μm. Parameters: $I_0 = e\Delta/\hbar$ and the rest as in Fig. 2.

exists only a small asymmetry with respect to $\phi = \pi$ in the quasicontinuum but no substantial effect is seen by naked eye at low energies [Figs. 2(a) and 2(b)]. Note that the Majorana zero-energy splitting gets suppressed as L_S increases, consistent with their inherent spatial nonlocality, see red curves in insets of Fig. 2(b); the ABSs for $B < B_c$ do not depend on L_S. In JJs with $L_N = 100$ nm the Andreev spectrum exhibits a stronger response to $\eta \neq 0$ [Figs. 2(c) and 2(d)]. While the trivial spectrum here is only weakly asymmetric [Fig. 2(c)], other values of L_N give spectra with larger asymmetries [89], see the Supplemental Material (SM) [90]. Irrespective of L_N, however, the asymmetric trivial Andreev spectrum does not depend on L_S because trivial ABSs are located only at the inner side of the JJ. In contrast, the Andreev spectrum for $B > B_c$ is more noticeable and strongly depends on L_S due to the presence of MBSs. In particular, the Majorana zero-energy splitting can occur at ϕ other than $\phi = \pi$ when $\eta \neq 0$ [Fig. 2(d)], thus showing the key role of $\mathbf{B}_N$ for inducing an asymmetric Andreev spectrum in topological JJs. Since the Majorana zero-energy splitting depends on L_S and $\eta \neq 0$, longer S regions give rise to four MBSs with zero energy, which then produce sharper zero-energy crossings that are asymmetric with respect to $\phi = \pi$, see insets in Fig. 2(d). As a result, finite topological JJs host a nonreciprocal length dependent Andreev spectrum entirely due to MBSs.

Nonreciprocal current-phase curves. Having established that the Andreev spectrum of JJs under Zeeman fields parallel to the SOC is asymmetric with respect to $\phi = \pi$, here we study how this asymmetry affects the supercurrents $I(\phi)$. At zero temperature, we obtain $I(\phi)$ as [34,70] $I(\phi) = -(e/\hbar)\sum_{\varepsilon_n>0}[d\,\varepsilon_n(\phi)/d\phi]$, where $\varepsilon_n(\phi)$ are the phase-dependent energy levels found in the previous section, which include the contribution of both the in-gap ABSs and the discrete quasicontinuum [71,72]. In Figs. 3(a)–3(c) we present $I(\phi)$ for JJs with $L_N = 100$ nm as a function of ϕ for different η and L_S in the trivial and topological phases. To better understand the role of MBSs, Fig. 3(d) shows the contribution of MBSs (I_{MBS}) and the rest of levels (I_{rest}) to the total $I(\phi)$; here I_{rest} includes the contribution due to the additional in-gap ABSs that coexist with MBSs and also of the quasicontinuum.

In Figs. 3(b) and 3(c) we see that $I(\phi)$ has an overall asymmetric profile with respect to $\phi = \pi$ at $\eta \neq 0$, which depends on η and B, and, importantly, with a distinct response in the trivial (topological) phase to changes in L_S. This asymmetric $I(\phi)$ at $\eta \neq 0$ is distinct to what is found at $\eta = 0$ [Fig. 3(a)], see also [70,88,91]. The weak (strong) asymmetry in $I(\phi)$ with respect to $\phi = \pi$ stems from the phase-dependent Andreev spectrum in Fig. 2, implying an important role of the in-gap ABSs and quasicontinuum. The trivial phase with $B < B_c$ shows a weak asymmetry for the chosen L_N due to the weakly asymmetric spectrum, but other values can give far more asymmetric $I(\phi)$. As a result of the asymmetry, $I(\phi)$ develops a global maximum that is distinct to its global minimum, namely, different critical currents $I_c^+ \neq I_c^-$, where $I_c^\pm = \max_\phi[\pm I(\phi)]$, see black arrow in Fig. 3(b). Another feature of this trivial phase is that $I(\phi)$ does not change when L_S increases for any η. This insensitivity originates from that the ABSs for $B < B_c$ emerge located at the inner sides of the JJ and thus do not depend on L_S, i.e., trivial ABSs are not spatially nonlocal.

In contrast to the trivial phase, in the topological phase with $B > B_c$, $I(\phi)$ forms a larger asymmetry with respect to $\phi = \pi$ and finite values at zero phase, which can be traced back to the Andreev spectrum Fig. 2(d). Interestingly, the asymmetry of $I(\phi)$ and $I_c^+ \neq I_c^-$ strongly depends on L_S, which is due to the presence of MBSs and different to what occurs for $B < B_c$. To see $I(\phi)$ with $I_c^+ \neq I_c^-$ we indicate with colored arrows the remaining difference between the two critical currents [Fig. 3(c)]; note that $I_c^+ = I_c^-$ for $\eta = 0$, as expected [Fig. 3(a)]. Interestingly, the regimes with $I_c^+ \neq I_c^-$ signal the emergence of nonreciprocal supercurrents, or JD effect, which here occurs in the trivial and, notably, also in the topological phases. While JDs in semiconductor-S hybrids have already been reported before [14,22,26,28,54–56], their emergence in topological JJs is intriguing because MBSs are naturally present in this regime. The effect of MBSs is evident by noting the strong dependence of $I_c^+ \neq I_c^-$ on L_S pointed out above. In fact, the topological phase hosts four spatially nonlocal MBSs exhibiting a zero-energy splitting at $\phi = \pi$ at $\eta = 0$ or away from π when $\eta \neq 0$ [Fig. 2(d)]. Then, by reducing the zero-energy Majorana splitting with increasing L_S, $I(\phi)$ acquires sharper sawtooth profiles, with larger differences between I_c^+ and I_c^- that can be easily distinguished from the trivial regime. The role of MBSs can be further seen in the individual contributions of the four MBSs and the rest of levels to the total $I(\phi)$ in Fig. 3(d). While I_{rest} has a sizable phase dependent value, the sharpness in the sawtooth profile of $I(\phi)$ (vertical dashed black line) is largely determined by I_{MBS} due to the reduction in the Majorana zero-energy splitting for large L_S. Hence, Majorana nonlocality plays a key role for enhancing the JD effect that has not been exploited before [81–86].

Critical currents and quality factors. To further understand and characterize the JDs found in previous section, here we

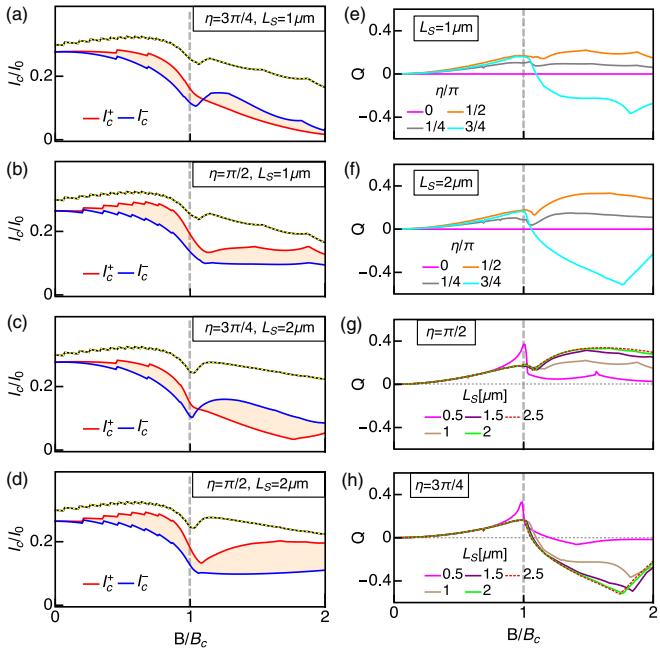

FIG. 4. Critical currents $I_c^{\pm}$ [(a)–(d)] and quality factors Q [(e)–(h)] as a function of the Zeeman field B in S for different η and L_S. The black-yellow curve in (a)–(d) shows the critical current at $\eta = 0$ where there is no diode effect. The vertical dashed-gray line marks the topological phase transition at $B = B_c$. Parameters: $L_N = 100$ nm and the rest as in Fig. 2.

show the critical currents I_c^+ and I_c^- and their quality factors $Q = (I_c^+ - I_c^-)/(I_c^+ + I_c^-)$. Having $Q \neq 0$ reveals the amount of nonreciprocity and a finite JD effect. In Figs. 4(a)–4(d) we show $I_c^{\pm}$ as a function of B for $\eta = \pi/2, 3\pi/4$ and distinct L_S, while in Figs. 4(e)–4(h) we present Q as a function of B. To contrast, we also plot $I_c^{\pm}$ at $\eta = 0$ in black-yellow curves of Figs. 4(a)–4(d). We immediately note that $\eta \neq 0$ induces $I_c^+ \neq I_c^-$, depicted by the shaded orange regions, thus highlighting the realization of JDs. We see that the JD requires a finite B in both cases $\eta = \pi/2, 3\pi/4$ for the chosen L_N but in the SM we show that it can already appear at $B = 0$ (see the SM [90]).

Both critical currents $I_c^{\pm}$ reduce as B increases but $I_c^+ \neq I_c^-$ persists and develop a kink at $B = B_c$, followed by finite values for $B > B_c$, see Figs. 4(a) and 4(b). Increasing L_S does not change the difference between $I_c^{\pm}$ for $B < B_c$, but, interestingly, it does $B > B_c$, inducing a larger nonreciprocity and the realization of enhanced JDs [Figs. 4(c) and 4(d)]. As discussed before, the sensitivity of the topological phase to changes in L_S is because this regime hosts spatially nonlocal MBSs, whose localization and zero-energy splitting strongly depends on L_S. Hence, we can conclude that the nonreciprocity in the critical currents, and their JDs, gets enhanced entirely due to the presence of MBSs, specially, due to its spatial nonlocality.

The nonreciprocity in $I_c^{\pm}$ gives rise to quality factors Q with a unique Zeeman dependence that confirms the impact of the nonlocal MBSs [Figs. 4(e)–4(h)]. At $\eta = 0$, $Q = 0$ due to $I_c^+ = I_c^-$, as expected, see magenta lines in Figs. 4(e) and 4(f). In contrast, at $\eta \neq 0$, Q gets finite values as B increases, exhibiting a peak at $B = B_c$ and finite values for $B > B_c$ that strongly depend on L_S [Figs. 4(e) and 4(f)]; see also SM [90]. These features are absent for $B < B_c$ and, hence, suggest a direct effect due to MBSs. To support this view, in Figs. 4(g) and 4(h) we show Q as a function of B at $\eta = \pi/2, 3\pi/4$ and distinct L_S. Here, Q for $B < B_c$ does not sense changes in L_S but it strongly reacts for $B > B_c$, developing higher values (see the SM [90]). The peak of Q at $B = B_c$ in Figs. 4(g) and 4(h) is due to the sharp Zeeman dependence of the ABS energies when the gap closing signals the topological phase transition. Since for $B > B_c$ the Majorana zero-energy splitting strongly depends on L_S, with vanishing values for long S, the response of Q to changes in L_S seen in Figs. 4(g) and 4(h) is only attributed to the Majorana nonlocality. Also, for certain η, Q changes sign only when $B > B_c$, showing that reversing the diode's polarity is intriguingly related to MBSs, see Figs. 4(e), 4(f), and 4(h) (see the SM [90]). Thus, topological JJs can notably realize JDs with larger quality factors due to the nonlocal nature of MBSs.

In conclusion, we studied Josephson diodes in finite topological Josephson junctions and found that their emergence is induced by having a Zeeman field in the normal region parallel and perpendicular to the spin-orbit coupling. We discovered that the quality factors of the Josephson diodes in the topological phase are greatly enhanced entirely due to the nonlocality of Majorana bound states, a mechanism that has not been explored before [81–86]. Similar Josephson junctions as those studied here based on superconductor-semiconductor hybrid systems have already been fabricated [14,22,43–45,48,49,54,92], which places our findings within experimental reach. Our results thus establish topological superconductivity for realizing topological Josephson diodes with protected and enhanced functionalities.

Acknowledgments. We thank Y. Asano, S. Ikegaya, and S. Tamura for insightful discussions. J.C. acknowledges support from the Japan Society for the Promotion of Science via the International Research Fellow Program, the Swedish Research Council (Vetenskapsrådet Grant No. 2021-04121), and the Carl Trygger's Foundation (Grant No. 22: 2093). N.N. acknowledges support from JST CREST Grant No. JPMJCR1874, Japan. Y.T. acknowledges support from JSPS with Grants-in-Aid for Scientific Research (KAKENHI Grants No. 20H00131 and No. 23K17668).

[1] L. A. Coldren, S. W. Corzine, and M. L. Mashanovitch, *Diode Lasers and Photonic Integrated Circuits* (John Wiley & Sons, Hoboken, NJ, 2012).

[2] I. Mehdi, J. V. Siles, C. Lee, and E. Schlecht, THz diode technology: Status, prospects, and applications, Proc. IEEE **105**, 990 (2017).

[3] J. Semple, D. G. Georgiadou, G. Wyatt-Moon, G. Gelinck, and T. D. Anthopoulos, Flexible diodes for radio frequency (RF) electronics: A materials perspective, Semicond. Sci. Technol. **32**, 123002 (2017).

[4] Y. Tokura and N. Nagaosa, Nonreciprocal responses from non-centrosymmetric quantum materials, Nat. Commun. **9**, 3740 (2018).

[5] M. Kim, E. Pallecchi, R. Ge, X. Wu, G. Ducournau, J. C. Lee, H. Happy, and D. Akinwande, Analogue switches made from boron nitride monolayers for application in 5G and terahertz communication systems, Nat. Electron. **3**, 479 (2020).

[6] K. Loganathan, H. Faber, E. Yengel, A. Seitkhan, A. Bakytbekov, E. Yarali, B. Adilbekova, A. AlBatati, Y. Lin, Z. Felemban *et al.*, Rapid and up-scalable manufacturing of gigahertz nanogap diodes, Nat. Commun. **13**, 3260 (2022).

[7] F. Braun, Ueber die stromleitung durch schwefelmetalle, Ann. Phys. **229**, 556 (1875).

[8] S. M. Sze and M.-K. Lee, *Semiconductor Devices: Physics and Technology* (Wiley, Hoboken, NJ, 2016).

[9] R. Wakatsuki, Y. Saito, S. Hoshino, Y. M. Itahashi, T. Ideue, M. Ezawa, Y. Iwasa, and N. Nagaosa, Nonreciprocal charge transport in noncentrosymmetric superconductors, Sci. Adv. **3**, e1602390 (2017).

[10] S. Hoshino, R. Wakatsuki, K. Hamamoto, and N. Nagaosa, Nonreciprocal charge transport in two-dimensional noncentrosymmetric superconductors, Phys. Rev. B **98**, 054510 (2018).

[11] K. Yasuda, H. Yasuda, T. Liang, R. Yoshimi, A. Tsukazaki, K. S. Takahashi, N. Nagaosa, M. Kawasaki, and Y. Tokura, Nonreciprocal charge transport at topological insulator/superconductor interface, Nat. Commun. **10**, 2734 (2019).

[12] F. Ando, Y. Miyasaka, T. Li, J. Ishizuka, T. Arakawa, Y. Shiota, T. Moriyama, Y. Yanase, and T. Ono, Observation of superconducting diode effect, Nature (London) **584**, 373 (2020).

[13] A. Daido, Y. Ikeda, and Y. Yanase, Intrinsic superconducting diode effect, Phys. Rev. Lett. **128**, 037001 (2022).

[14] Y. Hou, F. Nichele, H. Chi, A. Lodesani, Y. Wu, M. F. Ritter, D. Z. Haxell, M. Davydova, S. Ilić, O. Glezakou-Elbert, A. Varambally, F. S. Bergeret, A. Kamra, L. Fu, P. A. Lee, and J. S. Moodera, Ubiquitous superconducting diode effect in superconductor thin films, Phys. Rev. Lett. **131**, 027001 (2023).

[15] H. F. Legg, D. Loss, and J. Klinovaja, Superconducting diode effect due to magnetochiral anisotropy in topological insulators and Rashba nanowires, Phys. Rev. B **106**, 104501 (2022).

[16] J. J. He, Y. Tanaka, and N. Nagaosa, A phenomenological theory of superconductor diodes, New J. Phys. **24**, 053014 (2022).

[17] N. F. Yuan and L. Fu, Supercurrent diode effect and finite-momentum superconductors, Proc. Natl. Acad. Sci. USA **119**, e2119548119 (2022).

[18] J.-X. Lin, P. Siriviboon, H. D. Scammell, S. Liu, D. Rhodes, K. Watanabe, T. Taniguchi, J. Hone, M. S. Scheurer, and J. Li, Zero-field superconducting diode effect in small-twist-angle trilayer graphene, Nat. Phys. **18**, 1221 (2022).

[19] H. D. Scammell, J. Li, and M. S. Scheurer, Theory of zero-field superconducting diode effect in twisted trilayer graphene, 2D Mater. **9**, 025027 (2022).

[20] S. Banerjee and M. S. Scheurer, Enhanced superconducting diode effect due to coexisting phases, Phys. Rev. Lett. **132**, 046003 (2024).

[21] H. Wu, Y. Wang, Y. Xu, P. K. Sivakumar, C. Pasco, U. Filippozzi, S. S. Parkin, Y.-J. Zeng, T. McQueen, and M. N. Ali, The field-free Josephson diode in a van der Waals heterostructure, Nature (London) **604**, 653 (2022).

[22] C. Baumgartner, L. Fuchs, A. Costa, S. Reinhardt, S. Gronin, G. C. Gardner, T. Lindemann, M. J. Manfra, P. E. Faria, Jr., D. Kochan *et al.*, Supercurrent rectification and magnetochiral effects in symmetric Josephson junctions, Nat. Nanotechnol. **17**, 39 (2022).

[23] B. Pal, A. Chakraborty, P. K. Sivakumar, M. Davydova, A. K. Gopi, A. K. Pandeya, J. A. Krieger, Y. Zhang, M. Date, S. Ju *et al.*, Josephson diode effect from Cooper pair momentum in a topological semimetal, Nat. Phys. **18**, 1228 (2022).

[24] M. Davydova, S. Prembabu, and L. Fu, Universal Josephson diode effect, Sci. Adv. **8**, eabo0309 (2022).

[25] R. S. Souto, M. Leijnse, and C. Schrade, Josephson diode effect in supercurrent interferometers, Phys. Rev. Lett. **129**, 267702 (2022).

[26] A. Costa, J. Fabian, and D. Kochan, Microscopic study of the Josephson supercurrent diode effect in Josephson junctions based on two-dimensional electron gas, Phys. Rev. B **108**, 054522 (2023).

[27] J.-X. Hu, Z.-T. Sun, Y.-M. Xie, and K. T. Law, Josephson diode effect induced by valley polarization in twisted bilayer graphene, Phys. Rev. Lett. **130**, 266003 (2023).

[28] A. Maiani, K. Flensberg, M. Leijnse, C. Schrade, S. Vaitiekėnas, and R. Seoane Souto, Nonsinusoidal current-phase relations in semiconductor–superconductor–ferromagnetic insulator devices, Phys. Rev. B **107**, 245415 (2023).

[29] K. K. Likharev, Superconducting weak links, Rev. Mod. Phys. **51**, 101 (1979).

[30] M. Tinkham, *Introduction to Superconductivity* (Dover Publications, Mineola, NY, 2004).

[31] I. O. Kulik and A. N. Omel'yanchuk, Contribution to the microscopic theory of the Josephson effect in superconducting bridges, JETP Lett. **21**, 216 (1975).

[32] A. Furusaki and M. Tsukada, DC Josephson effect and Andreev reflection, Solid State Commun. **78**, 299 (1991).

[33] A. Furusaki, H. Takayanagi, and M. Tsukada, Josephson effect of the superconducting quantum point contact, Phys. Rev. B **45**, 10563 (1992).

[34] C. Beenakker, Three "universal" mesoscopic Josephson effects, in *Transport Phenomena in Mesoscopic Systems: Proceedings of the 14th Taniguchi Symposium, Shima, Japan, 10-14 November, 1991*, Vol. 109 (Springer-Verlag, Berlin, 1992) p. 235.

[35] A. Furusaki, Josephson current carried by Andreev levels in superconducting quantum point contacts, Superlattices Microstruct. **25**, 809 (1999).

[36] S. Kashiwaya and Y. Tanaka, Tunnelling effects on surface bound states in unconventional superconductors, Rep. Prog. Phys. **63**, 1641 (2000).

[37] Y. Asano, Direct-current Josephson effect in SNS junctions of anisotropic superconductors, Phys. Rev. B **64**, 224515 (2001).

[38] Y. Asano, Y. Tanaka, and S. Kashiwaya, Anomalous Josephson effect in *p*-wave dirty junctions, Phys. Rev. Lett. **96**, 097007 (2006).

[39] A. A. Golubov, M. Y. Kupriyanov, and E. Il'ichev, The current-phase relation in Josephson junctions, Rev. Mod. Phys. **76**, 411 (2004).

[40] J. Sauls, Andreev bound states and their signatures, Philos. Trans. Royal Soc. A **376**, 20180140 (2018).

[41] T. Mizushima and K. Machida, Multifaceted properties of Andreev bound states: Interplay of symmetry and topology, Philos. Trans. R. Soc. A **376**, 20150355 (2018).

[42] Y. Tanaka, M. Sato, and N. Nagaosa, Symmetry and topology in superconductors–odd-frequency pairing and edge states, J. Phys. Soc. Jpn. **81**, 011013 (2012).

[43] J. Tiira, E. Strambini, M. Amado, S. Roddaro, P. San-Jose, R. Aguado, F. S. Bergeret, D. Ercolani, L. Sorba, and F. Giazotto, Magnetically-driven colossal supercurrent enhancement in InAs nanowire Josephson junctions, Nat. Commun. **8**, 14984 (2017).

[44] M. Hays, G. de Lange, K. Serniak, D. J. van Woerkom, D. Bouman, P. Krogstrup, J. Nygård, A. Geresdi, and M. H. Devoret, Direct microwave measurement of Andreev-bound-state dynamics in a semiconductor-nanowire Josephson junction, Phys. Rev. Lett. **121**, 047001 (2018).

[45] L. Tosi, C. Metzger, M. F. Goffman, C. Urbina, H. Pothier, S. Park, A. L. Yeyati, J. Nygård, and P. Krogstrup, Spin-orbit splitting of Andreev states revealed by microwave spectroscopy, Phys. Rev. X **9**, 011010 (2019).

[46] H. Ren, F. Pientka, S. Hart, A. T. Pierce, M. Kosowsky, L. Lunczer, R. Schlereth, B. Scharf, E. M. Hankiewicz, L. W. Molenkamp *et al.*, Topological superconductivity in a phase-controlled Josephson junction, Nature (London) **569**, 93 (2019).

[47] A. Fornieri, A. M. Whiticar, F. Setiawan, E. Portolés, A. C. C. Drachmann, A. Keselman, S. Gronin, C. Thomas, T. Wang, R. Kallaher *et al.*, Evidence of topological superconductivity in planar Josephson junctions, Nature (London) **569**, 89 (2019).

[48] F. Nichele, E. Portolés, A. Fornieri, A. M. Whiticar, A. C. C. Drachmann, S. Gronin, T. Wang, G. C. Gardner, C. Thomas, A. T. Hatke, M. J. Manfra, and C. M. Marcus, Relating Andreev bound states and supercurrents in hybrid Josephson junctions, Phys. Rev. Lett. **124**, 226801 (2020).

[49] D. Razmadze, E. C. T. O'Farrell, P. Krogstrup, and C. M. Marcus, Quantum dot parity effects in trivial and topological Josephson junctions, Phys. Rev. Lett. **125**, 116803 (2020).

[50] R. M. Lutchyn, E. P. Bakkers, L. P. Kouwenhoven, P. Krogstrup, C. M. Marcus, and Y. Oreg, Majorana zero modes in superconductor–semiconductor heterostructures, Nat. Rev. Mater. **3**, 52 (2018).

[51] E. Prada, P. San-Jose, M. W. de Moor, A. Geresdi, E. J. Lee, J. Klinovaja, D. Loss, J. Nygård, R. Aguado, and L. P. Kouwenhoven, From Andreev to Majorana bound states in hybrid superconductor–semiconductor nanowires, Nat. Rev. Phys. **2**, 575 (2020).

[52] S. M. Frolov, M. J. Manfra, and J. D. Sau, Topological superconductivity in hybrid devices, Nat. Phys. **16**, 718 (2020).

[53] K. Flensberg, F. von Oppen, and A. Stern, Engineered platforms for topological superconductivity and Majorana zero modes, Nat. Rev. Mater. **6**, 944 (2021).

[54] G. P. Mazur, N. van Loo, D. van Driel, J. Y. Wang, G. Badawy, S. Gazibegovic, E. P. A. M. Bakkers, and L. P. Kouwenhoven, The gate-tunable Josephson diode, arXiv:2211.14283.

[55] M. Nadeem, M. S. Fuhrer, and X. Wang, The superconducting diode effect, Nat. Rev. Phys. **5**, 558 (2023).

[56] M. Valentini, O. Sagi, L. Baghumyan, T. de Gijsel, J. Jung, S. Calcaterra, A. Ballabio, J. A. Servin, K. Aggarwal, M. Janik *et al.*, Parity-conserving cooper-pair transport and ideal superconducting diode in planar germanium, Nat. Commun. **15**, 169 (2024).

[57] X.-L. Qi and S.-C. Zhang, Topological insulators and superconductors, Rev. Mod. Phys. **83**, 1057 (2011).

[58] M. Leijnse and K. Flensberg, Introduction to topological superconductivity and Majorana fermions, Semicond. Sci. Technol. **27**, 124003 (2012).

[59] C. Beenakker, Search for Majorana fermions in superconductors, Annu. Rev. Condens. Matter Phys. **4**, 113 (2013).

[60] M. Sato and Y. Ando, Topological superconductors: A review, Rep. Prog. Phys. **80**, 076501 (2017).

[61] P. Marra, Majorana nanowires for topological quantum computation, J. Appl. Phys. **132**, 231101 (2022).

[62] L. Fu and C. L. Kane, Superconducting proximity effect and Majorana fermions at the surface of a topological insulator, Phys. Rev. Lett. **100**, 096407 (2008).

[63] M. Sato, Y. Takahashi, and S. Fujimoto, Non-Abelian topological order in *s*-wave superfluids of ultracold fermionic atoms, Phys. Rev. Lett. **103**, 020401 (2009).

[64] Y. Tanaka, T. Yokoyama, and N. Nagaosa, Manipulation of the Majorana fermion, Andreev reflection, and Josephson current on topological insulators, Phys. Rev. Lett. **103**, 107002 (2009).

[65] Y. Oreg, G. Refael, and F. von Oppen, Helical liquids and Majorana bound states in quantum wires, Phys. Rev. Lett. **105**, 177002 (2010).

[66] R. M. Lutchyn, J. D. Sau, and S. Das Sarma, Majorana fermions and a topological phase transition in semiconductor-superconductor heterostructures, Phys. Rev. Lett. **105**, 077001 (2010).

[67] P. San-Jose, E. Prada, and R. Aguado, ac Josephson effect in finite-length nanowire junctions with Majorana modes, Phys. Rev. Lett. **108**, 257001 (2012).

[68] J. Cayao, E. Prada, P. San-Jose, and R. Aguado, SNS junctions in nanowires with spin-orbit coupling: Role of confinement and helicity on the subgap spectrum, Phys. Rev. B **91**, 024514 (2015).

[69] Y. Peng, F. Pientka, E. Berg, Y. Oreg, and F. von Oppen, Signatures of topological Josephson junctions, Phys. Rev. B **94**, 085409 (2016).

[70] J. Cayao, P. San-Jose, A. M. Black-Schaffer, R. Aguado, and E. Prada, Majorana splitting from critical currents in Josephson junctions, Phys. Rev. B **96**, 205425 (2017).

[71] J. Cayao, A. M. Black-Schaffer, E. Prada, and R. Aguado, Andreev spectrum and supercurrents in nanowire-based SNS junctions containing Majorana bound states, Beilstein J. Nanotechnol. **9**, 1339 (2018).

[72] J. Cayao and A. M. Black-Schaffer, Distinguishing trivial and topological zero-energy states in long nanowire junctions, Phys. Rev. B **104**, L020501 (2021).

[73] B. Pekerten, J. D. Pakizer, B. Hawn, and A. Matos-Abiague, Anisotropic topological superconductivity in Josephson junctions, Phys. Rev. B **105**, 054504 (2022).

[74] L. Baldo, L. G. D. Da Silva, A. M. Black-Schaffer, and J. Cayao, Zero-frequency supercurrent susceptibility signatures of trivial and topological zero-energy states in nanowire junctions, Supercond. Sci. Technol. **36**, 034003 (2023).

[75] Y. Tanaka, S. Tamura, and J. Cayao, Theory of Majorana zero modes in unconventional superconductors, arXiv:2402.00643.

[76] S. D. Sarma, M. Freedman, and C. Nayak, Majorana zero modes and topological quantum computation, npj Quantum Inf. **1**, 15001 (2015).

[77] V. Lahtinen and J. K. Pachos, A short introduction to topological quantum computation, SciPost Phys. **3**, 021 (2017).

[78] C. W. J. Beenakker, Search for non-Abelian Majorana braiding statistics in superconductors, SciPost Phys. Lect. Notes, 15 (2020).

[79] R. Aguado and L. P. Kouwenhoven, Majorana qubits for topological quantum computing, Phys. Today **73**(6), 44 (2020).

[80] R. Aguado, A perspective on semiconductor-based superconducting qubits, Appl. Phys. Lett. **117**, 240501 (2020).

[81] T. Karabassov, I. V. Bobkova, A. A. Golubov, and A. S. Vasenko, Hybrid helical state and superconducting diode effect in superconductor/ferromagnet/topological insulator heterostructures, Phys. Rev. B **106**, 224509 (2022).

[82] Y. Tanaka, B. Lu, and N. Nagaosa, Theory of giant diode effect in d-wave superconductor junctions on the surface of a topological insulator, Phys. Rev. B **106**, 214524 (2022).

[83] P.-H. Fu, Y. Xu, C. H. Lee, S. A. Yang, Y. S. Ang, and J.-F. Liu, Field-effect Josephson diode via asymmetric spin-momentum locking states, arXiv:2212.01980.

[84] H. F. Legg, K. Laubscher, D. Loss, and J. Klinovaja, Parity protected superconducting diode effect in topological Josephson junctions, arXiv:2301.13740.

[85] B. Lu, S. Ikegaya, P. Burset, Y. Tanaka, and N. Nagaosa, Tunable Josephson diode effect on the surface of topological insulators, Phys. Rev. Lett. **131**, 096001 (2023).

[86] J. J. Cuozzo, W. Pan, J. Shabani, and E. Rossi, Microwave-tunable diode effect in asymmetric squids with topological Josephson junctions, arXiv:2303.16931.

[87] The Zeeman field in N can be induced by coupling N to distinct ferromagnets [93–97], by depositing distinct magnetic atoms [98–101], or by a 3D vector magnet attached only to N [49,102–104].

[88] O. A. Awoga, J. Cayao, and A. M. Black-Schaffer, Supercurrent detection of topologically trivial zero-energy states in nanowire junctions, Phys. Rev. Lett. **123**, 117001 (2019).

[89] T. Yokoyama, M. Eto, and Y. V. Nazarov, Anomalous Josephson effect induced by spin-orbit interaction and Zeeman effect in semiconductor nanowires, Phys. Rev. B **89**, 195407 (2014).

[90] See Supplemental Material at http://link.aps.org/supplemental/10.1103/PhysRevB.109.L081405 for additional calculations supporting our main findings. In particular, we present calculations of the spectra, critical currents, and quality factors for distinct values of the lengths of the N and S regions.

[91] J. Cayao and A. M. Black-Schaffer, Finite length effect on supercurrents between trivial and topological superconductors, Eur. Phys. J.: Spec. Top. **227**, 1387 (2018).

[92] E. M. Spanton, M. Deng, S. Vaitiekėnas, P. Krogstrup, J. Nygård, C. M. Marcus, and K. A. Moler, Current–phase relations of few-mode InAs nanowire Josephson junctions, Nat. Phys. **13**, 1177 (2017).

[93] Y. Liu, S. Vaitiekenas, S. Martí-Sánchez, C. Koch, S. Hart, Z. Cui, T. Kanne, S. A. Khan, R. Tanta, S. Upadhyay *et al.*, Semiconductor–ferromagnetic insulator–superconductor nanowires: Stray field and exchange field, Nano Lett. **20**, 456 (2020).

[94] S. Vaitiekėnas, Y. Liu, P. Krogstrup, and C. Marcus, Zero-bias peaks at zero magnetic field in ferromagnetic hybrid nanowires, Nat. Phys. **17**, 43 (2021).

[95] S. D. Escribano, A. Maiani, M. Leijnse, K. Flensberg, Y. Oreg, A. Levy Yeyati, E. Prada, and R. Seoane Souto, Semiconductor-ferromagnet-superconductor planar heterostructures for 1D topological superconductivity, npj Quantum Mater. **7**, 81 (2022).

[96] S. Vaitiekėnas, R. S. Souto, Y. Liu, P. Krogstrup, K. Flensberg, M. Leijnse, and C. M. Marcus, Evidence for spin-polarized bound states in semiconductor–superconductor–ferromagnetic-insulator islands, Phys. Rev. B **105**, L041304 (2022).

[97] D. Razmadze, R. S. Souto, L. Galletti, A. Maiani, Y. Liu, P. Krogstrup, C. Schrade, A. Gyenis, C. M. Marcus, and S. Vaitiekėnas, Supercurrent reversal in ferromagnetic hybrid nanowire Josephson junctions, Phys. Rev. B **107**, L081301 (2023).

[98] S. Nadj-Perge, I. K. Drozdov, J. Li, H. Chen, S. Jeon, J. Seo, A. H. MacDonald, B. A. Bernevig, and A. Yazdani, Observation of Majorana fermions in ferromagnetic atomic chains on a superconductor, Science **346**, 602 (2014).

[99] L. Farinacci, G. Ahmadi, G. Reecht, M. Ruby, N. Bogdanoff, O. Peters, B. W. Heinrich, F. von Oppen, and K. J. Franke, Tuning the coupling of an individual magnetic impurity to a superconductor: Quantum phase transition and transport, Phys. Rev. Lett. **121**, 196803 (2018).

[100] E. Liebhaber, L. M. Rütten, G. Reecht, J. F. Steiner, S. Rohlf, K. Rossnagel, F. von Oppen, and K. J. Franke, Quantum spins and hybridization in artificially-constructed chains of magnetic adatoms on a superconductor, Nat. Commun. **13**, 2160 (2022).

[101] M. Trahms, L. Melischek, J. F. Steiner, B. Mahendru, I. Tamir, N. Bogdanoff, O. Peters, G. Reecht, C. B. Winkelmann, F. von Oppen, and K. J. Franke, Diode effect in Josephson junctions with a single magnetic atom, Nature (London) **615**, 628 (2023).

[102] V. Mourik, K. Zuo, S. M. Frolov, S. Plissard, E. P. Bakkers, and L. P. Kouwenhoven, Signatures of Majorana fermions in hybrid superconductor-semiconductor nanowire devices, Science **336**, 1003 (2012).

[103] Q. Wang, S. L. Ten Haaf, I. Kulesh, D. Xiao, C. Thomas, M. J. Manfra, and S. Goswami, Triplet correlations in Cooper pair splitters realized in a two-dimensional electron gas, Nat. Commun. **14**, 4876 (2023).

[104] A. Bordin, G. Wang, C.-X. Liu, S. L. D. ten Haaf, N. van Loo, G. P. Mazur, D. Xu, D. van Driel, F. Zatelli, S. Gazibegovic, G. Badawy, E. P. A. M. Bakkers, M. Wimmer, L. P. Kouwenhoven, and T. Dvir, Tunable crossed Andreev reflection and elastic cotunneling in hybrid nanowires, Phys. Rev. X **13**, 031031 (2023).